Available online at www.sciencedirect.com
SCIENCE DIRECT®
ELSEVIER
Journal of Nuclear Materials 319 (2003) 95–101
journal of nuclear materials
www.elsevier.com/locate/jnucmat

Morphology change of rock-like oxide fuels in reactivity-initiated-accident simulation tests

T. Nakamura *, H. Sasajima, T. Yamashita, H. Uetsuka

Department of Reactor Safety Research, Japan Atomic Energy Research Institute, Tokai-mura, Ibaraki-ken 319-1195, Japan

Abstract

Pulse irradiation tests under simulated reactivity-initiated accident (RIA) conditions were performed with three types of rock-like oxide (ROX) fuels. Single phase yttria stabilized zirconia (YSZ), homogeneous mixture of YSZ/spinel and YSZ particle dispersed in spinel type ROX fuels were pulse irradiated in the Nuclear Safety Research Reactor (NSRR). Mode and threshold of the fuel rod failure including its consequences were investigated under the RIA conditions. The cladding failure occurred in a burst type mode in all the three types of ROX fuel tests with considerable fuel melting. Even though the mode was quite different from those of UO_2 fuel, failure threshold enthalpies of the ROX fuels were close to that of UO_2 fuel at about 10 $GJ\,m^{-3}$. The consequence of the failure of the ROX fuels rods was different from the one of UO_2 fuel rods, because molten fuel dispersal occurred at lower enthalpies in the ROX fuel tests. Change of the fuel structure and material interaction in the transient heating conditions were examined through optical and secondary electron microscopy, and electron probe micro analysis.

1. Introduction

As an optional method for burning excess plutonium (Pu) in light water reactors (LWRs), utilization of rock-like oxide (ROX) fuel has been proposed [1]. The fuel contains Pu in rock-like stable compounds, which is inert from a nuclear point of view. Yttria stabilized zirconia (YSZ: $Y_{0.2}Zr_{0.8}O_{1.9}$) was chosen as a host material for Pu and spinel ($MgAl_2O_4$) was mixed to improve thermal conductivity of the fuel. The ROX fuel could burn Pu almost completely, because it has practically no fertile ^{238}U. The absence of the fertile material, however, would cause quite small Doppler reactivity feedback and would result in quite high fuel enthalpies in reactivity-initiated accidents (RIAs). Therefore, some remedies for improving the coefficient are considered. Addition of resonant nuclides such as ^{232}Th or ^{238}U to the ROX fuel, or heterogeneous core configuration with UO_2 fuel could be practical candidate for the purpose [2]. In addition, the ROX fuels have different properties from those of UO_2 fuels in many respects, e.g. melting temperature, density, thermal conductivity and thermal expansion coefficient [3]. Thus, their behavior under the RIA conditions must be investigated to examine their feasibility in LWRs and to optimize their Pu transmutation and RIA resistant characteristics. Three types of the ROX fuels were pulse irradiated in the Nuclear Safety Research Reactor (NSRR) in order to investigate their behavior under the RIA conditions. Fuel rod failure thresholds were examined in the study and reported earlier [4–6]. This paper describes fuel material interactions and morphology changes in the fast thermal transient conditions, which are important for the failure behavior as well as for its consequences.

2. Test fuel rods

Three kinds of ROX fuel pellets were assembled into 17×17 PWR type short fuel rods of a stack length of

* Corresponding author. Tel.: +81-29 282 6386; fax: +81-29 282 5429.
E-mail address: take@fsrl.tokai.jaeri.go.jp (T. Nakamura).

0022-3115/03/$ - see front matter © 2003 Elsevier Science B.V. All rights reserved.
doi:10.1016/S0022-3115(03)00139-9

Table 1
Specifications of ROX test fuel rod

	Item		Specifications
Fuel pellet	^{235}U enrichment (wt%)		19.5
	Diameter and Length (mm)		8.05 and 9.0
	Material composition (mol%)	Single phase	$Y_{0.16}U_{0.20}Zr_{0.8}O_{1.9}$
		Mixed	$Y_{0.15}U_{0.50}Zr_{0.35}O_{1.93}$:$MgAl_2O_4$ = 52:48
		Dispersed	$Y_{0.07}U_{0.65}Zr_{0.28}O_{1.96}$:$MgAl_2O_4$ = 57:43
	Density (kg m^{-3})	Single phase	6.0×10^3
		Mixed	5.6×10^3
		Dispersed	5.5×10^3
Cladding	Material		Zircaloy-4
	Outer diameter (mm)		9.5
	Inner diameter (mm)		8.22 (thickness: 0.64)
Element	Pellet-cladding radial gap (mm)		0.085
	Total and stack length (mm)		279 and 135

135 mm. The rods contained 15 ROX fuel pellets sheathed in a Zircaloy-4 cladding. Diameter of the cladding and pellets were 9.5 and 8.05 mm, respectively. Three types of ROX pellets are

(1) Single phase type: single phase solid solution of UO_2 and yttria stabilized zirconia (YSZ): $Y_{0.16}U_{0.20}Zr_{0.64}O_{1.92}$.
(2) Mixed type: finely mixed two phase composite of $Y_{0.15}U_{0.5}Zr_{0.35}O_{1.93}$ and $MgAl_2O_4$, and
(3) Dispersed type: composite of larger $Y_{0.07}U_{0.65}Zr_{0.28}O_{1.96}$ sphere particles (diameter: about 0.3 mm) dispersed in $MgAl_2O_4$ matrix.

Plutonium was replaced by uranium for easier handling. Changes in the mechanical and thermal properties by the replacement were examined to be quite limited [3]. Material compositions of three types of ROX fuels are summarized in Table 1. Enrichment of ^{235}U was 19.5 wt% in all the ROX fuels.

3. Test procedure

The test fuel rods, contained in experimental capsules filled with water at room temperature and at ambient pressure were pulse irradiated in the NSRR. The rods were subjected to prompt thermal energies from 3.2 to 12.4 GJ m^{-3} (0.5–2.2 kJ g^{-1}) within short power pulses of full widths at half maximum from 4.5 to 14 ms in nine tests. Test conditions are listed in Table 2. Transient behavior of the rods was monitored through measurements with thermocouples, elongation sensors for pellet stack and cladding, strain gages for cladding hoop strain, and fuel rod internal pressure sensors. Change of the fuel microstructure was examined by optical

Table 2
Conditions and results of ROX fuel pulse irradiation tests

Fuel type	Test ID								
	Single phase			Mixed			Dispersed		
	945-1	945-2	945-3	943-1	943-2	943-3	947-1	947-2	947-3
Fuel enthalpy (GJ m^{-3})[a]	3.2	9.0	11.5	5.6	9.1	12.4	8.9	12.2	10.5
Fuel enthalpy (kJ g^{-1})[a]	0.5	1.5	1.9	1.0	1.6	2.2	1.6	2.2	1.9
Fuel temperature (K)[b]	1770	2820	2940	1890	2210	2210	2210	2210	2210
Fuel melt fraction (%)[b]	0	35	84	0	14	55	8	54	29
Cladding surface temperature (K)[a]	450	1650	1850	1100	1450	1750	1400	1650	1630
Failure	No	No	Yes	No	No	Yes	No	Yes	Yes
Fuel dispersed (%)	–	–	50	–	–	70	–	78	36

[a] Peak during the transient.
[b] Peak during the transient calculated with FRAP-T6 [6,7,9].

microscopy, scanning electron microscopy (SEM) and electron probe microanalysis (EPMA).

4. Test results and discussion

4.1. Transient behavior

By the pulse irradiation, test fuel rods was promptly heated up and the cladding surface temperature rose up as high as 1850 K depending on the fuel enthalpies, as shown in Fig. 1 for the tests with the Single phase fuels. Fuel was calculated to reach their melting temperatures and the melt fraction was as high as 84% [6]. Fuel melting temperature of the single phase $Y_{0.16}U_{0.20}Zr_{0.64}O_{1.92}$ and the composites with $MgAl_2O_4$ are 3000 and 2206 K (eutectic), respectively, while that of UO_2 is 3110 K. Peak cladding temperature was primarily a function of volumetric fuel enthalpy, regardless to the variety of the fuel pellets with various properties, as indicated in Fig. 2 [6]. Cladding failure occurred in four ROX fuel tests, in which cladding surface temperature reached to about 1600 K or higher at volumetric fuel enthalpies of about 10 $GJ\,m^{-3}$ or higher. The results suggested that the failure occurred if the cladding temperature reached close to its melting temperature and had lost its mechanical strength to a large extent. Accordingly, the failure threshold enthalpies were similar among all the ROX fuels and even with UO_2 fuel. Cladding failure enthalpy of fresh UO_2 fuel rod is 9.2 $GJ\,m^{-3}$ (0.89 $kJ\,g^{-1}$) [7]. Main test results are summarized in Table 2.

Consequence of the fuel rod failure, however, was quite different in the ROX fuel tests from that in UO_2 fuel test. Because of the lower fuel melting temperatures of the ROX fuels, considerable fraction of the fuel was molten by the time of failure and it was released to the surrounding water. The released fuel was fragmented into fine pieces. Example of the fuel cross-sections and fuel fragments are assembled in Fig. 3. The UO_2 fuel, on the other hand, stays solid at the corresponding volumetric enthalpy.

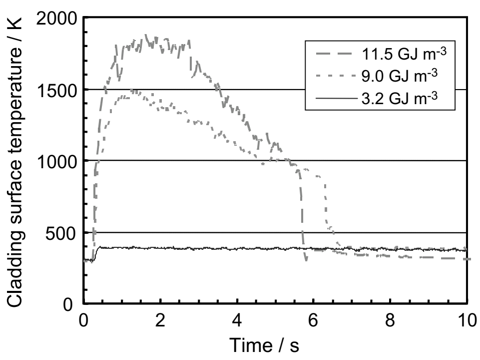

Fig. 1. Cladding surface temperature histories in the single phase type ROX fuel tests.

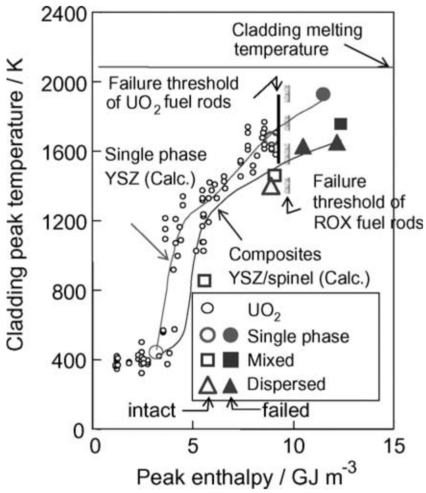

Fig. 2. Peak cladding surface temperature in three types of ROX fuels in comparison with UO_2 fuel. Peak cladding temperature for the Single phase and composite type ROX fuels are calculated with FRAP-T6 code.

4.2. Change in fuel microstructure

Because the interaction of YSZ and spinel and resulting fuel melting are important characteristics of the ROX fuel behavior during the transient heating tests, microstructure change of the fuels was examined by the SEM/EPMA.

4.2.1. Single phase type ROX fuel

Elemental analysis of the pre-test fuel pellet indicated that uranium rich islands of about 30 μm are uniformly distributed in the YSZ matrix. The fuel microstructure did not indicate significant change in the tests, except for that at the highest fuel enthalpy of 11.5 $GJ\,m^{-3}$. In the test, 84% of the fuel was calculated [6,7] to be molten and considerable interaction of the fuel with the cladding was observed. As a result of the cladding failure, about 50% of fuel was released to surrounding water. Size distribution of the fuel fragments is illustrated in Fig. 4. Average size of the single phase ROX fuel fragments was larger than 1 mm. That was much larger than those observed in the fresh [10] and irradiated [11,12] UO_2 fuel tests, which resulted in the pressure pulse and water hammer generation due to molten fuel and coolant interaction (FCI).

In the UO_2 fuel tests at peak fuel enthalpies of about 12 $GJ\,m^{-3}$ (1.2 $kJ\,g^{-1}$) or higher, instantaneous dispersion of molten fuel and subsequent fine fragmentation

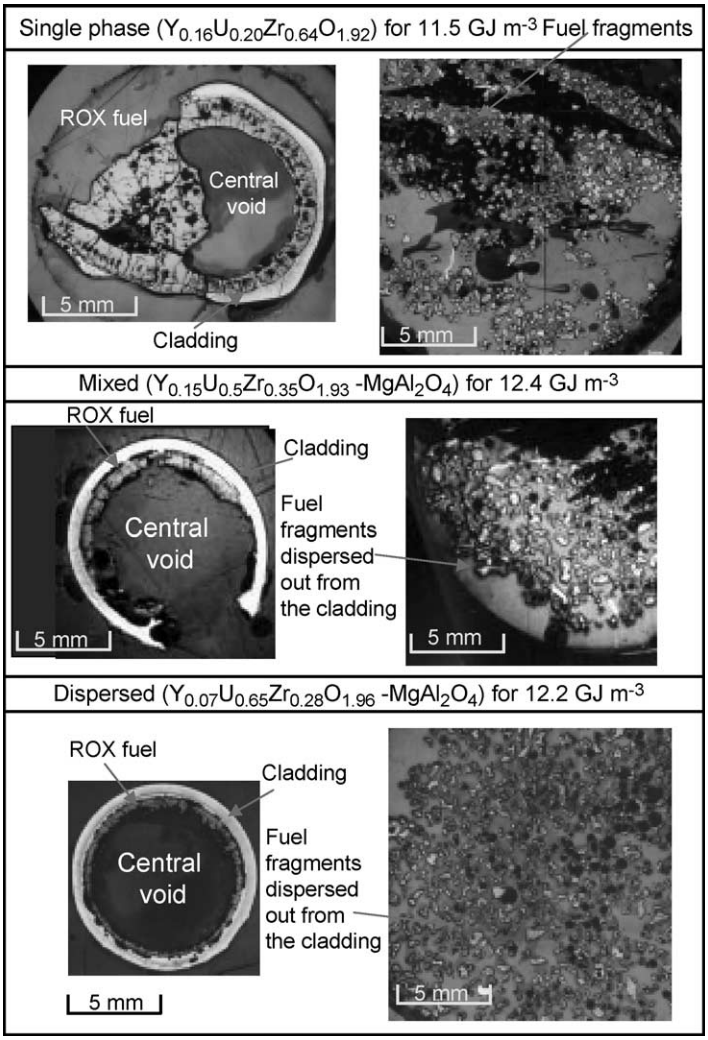

Fig. 3. Examples of fuel cross sections and fuel fragments failed in the NSRR ROX fuel tests.

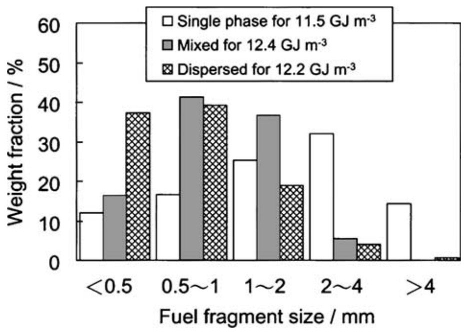

Fig. 4. Size distribution of three types of ROX fuel fragments failed at peak fuel enthalpies of about 12 GJ m^{-3}.

resulted in coherent generation of vapor in the test capsule. Upper part of the water in the capsule was, then, accelerated upward by the vapor, as illustrated in Fig. 5. In order to avoid this water hammer due to FCI and to maintain coolable geometry in the reactor, fuel enthalpy limits were defined in safety evaluation guidelines of many countries [13], in addition to the fuel rod failure criteria. The peak fuel enthalpies must be within the limits even in the worst design base RIAs. In the UO_2 fuel tests which resulted in significant FCI, the mean diameter of the fuel fragments was about 0.1 mm or smaller.

Even though the significant molten fuel release, water hammer due to the FCI was not observed in any of the ROX fuel tests through measurements of water level by a float. Smaller surface to volume ratio, due to the larger size of the ROX fuel fragments, should have contributed to the mild failure behavior. Spherical shell-like fuel fragments with large central voids, which were important

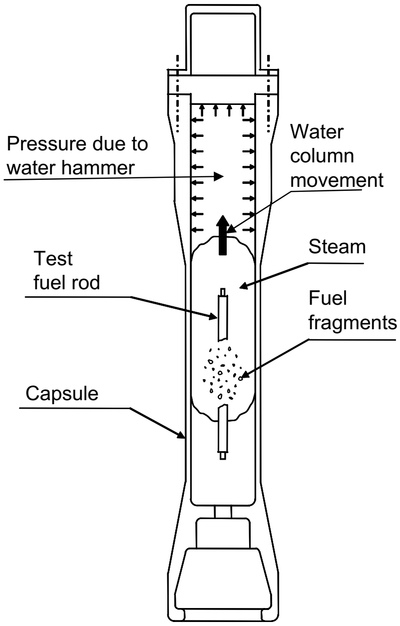

Fig. 5. Schematic illustration of water hammer generation due to fuel–coolant interaction by fuel rod failure and fuel dispersion in the NSRR irradiation capsule.

characteristics of the UO_2 fragments with the FCI [10], were rarely seen in the ROX fuels, as shown in Fig. 3.

4.2.2. Mixed type ROX fuel

In this type of ROX fuel, $Y_{0.15}U_{0.5}Zr_{0.35}O_{1.93}$ islands of about 10 μm are uniformly distributed in the spinel matrix, as shown in Fig. 6. Signs of the $Y_{0.15}U_{0.5}Zr_{0.35}O_{1.93}$ and spinel interaction were observed in a test at a peak fuel enthalpy of 9.1 $GJ\,m^{-3}$, where 14% of the fuel was calculated to be once molten [8]. In the other test at a higher enthalpy of 12.4 $GJ\,m^{-3}$ where 55% of the fuel was once molten, white $Y_{0.15}U_{0.5}Zr_{0.35}O_{1.93}$ was dispersed finely over the spinel matrix and uranium rich dendrite structure was observed in the post-test micrographs. Even though the melt fraction was smaller in the Mixed type fuel than in the single phase fuel, a larger fraction of about 70% of the fuel was released out from the failed cladding. The average size of the fragments was slightly smaller in the Mixed type fuel, as illustrated in Fig. 4. The fuel–coolant interaction, however, was not observed in this type of fuel tests, as well. Spherical shell-like fuel fragments, indicating the FCI, were not evident.

4.2.3. Dispersed type ROX fuel

Interaction of $Y_{0.07}U_{0.65}Zr_{0.28}O_{1.96}$ particles with spinel matrix was evident at peak fuel enthalpies above

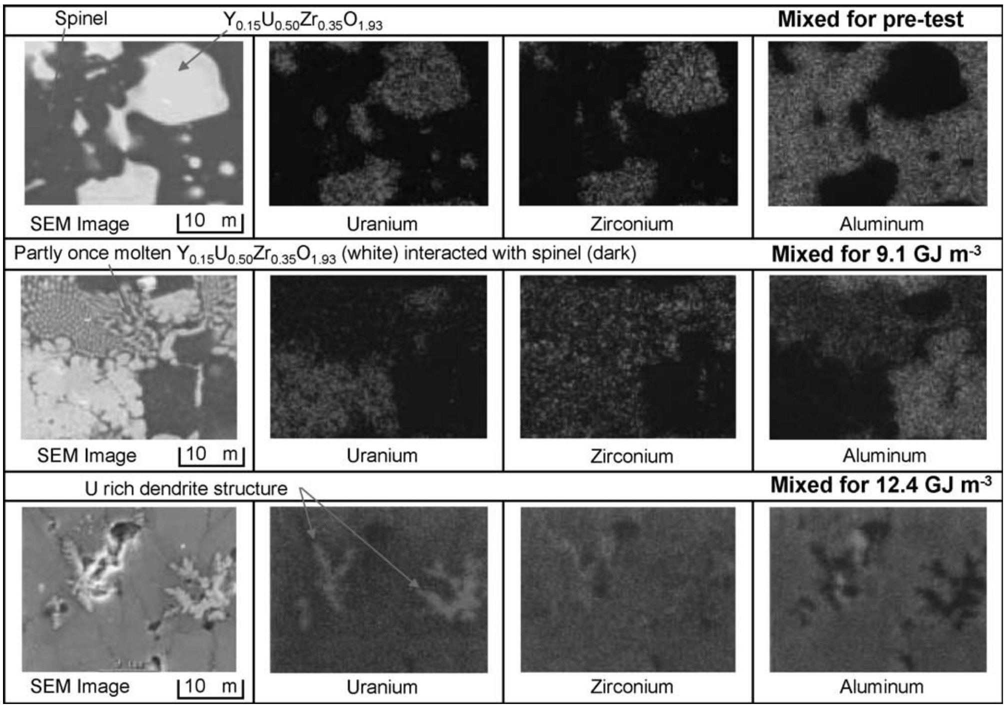

Fig. 6. Microstructure of the Mixed type ROX fuel before and after the pulse irradiation tests. Interaction of $Y_{0.15}U_{0.50}Zr_{0.35}O_{1.93}$ and spinel ($MgAl_2O_4$) was observed in the tests at peak fuel enthalpies of 9.1 $GJ\,m^{-3}$ or higher.

8.9 GJ m^{-3}, as shown in Fig. 7. As shown in macroscopic photos in Fig. 7, the interaction became heavier and fuel part looked more uniform as the fuel enthalpy went higher. A fairly large central void was generated as a result of fuel melting and its release at peak fuel enthalpies above 10.5 GJ m^{-3}. Fuel-cladding chemical interaction was evident only in the highest fuel enthalpy test, where cladding temperature rose up close to its melting temperature. Micrographs of the once molten fuel exhibited dendrite structure similar to those observed in the Mixed type fuel.

In the dispersed fuel fragments, once molten $Y_{0.07}U_{0.65}Zr_{0.28}O_{1.96}$ and spinel were distributed fairly uniformly. The fragment size of the dispersed type was the smallest of all the ROX fuels, as shown in Fig. 4. Slightly higher initial rod internal pressure of 0.4 MPa (0.1 MPa in other tests) in the dispersed type rods could have contributed to the slightly finer fragmentation and larger release of molten fuel of 78%, at a comparable peak fuel enthalpy of 12.2 GJ m^{-3} to that of the mixed type. Mechanical energy generation due to the FCI, however, was not observed in the severest test of the ROX fuel. Hydrodynamic effect in the high pressurized fuel rods was known to enhance mixing of the molten fuel and the coolant [10]. Though, it was not strong enough to cause the FCI in the present ROX fuel tests. Lower melting temperature of the ROX fuels than that of UO_2 makes the differential temperature to the coolant smaller. This

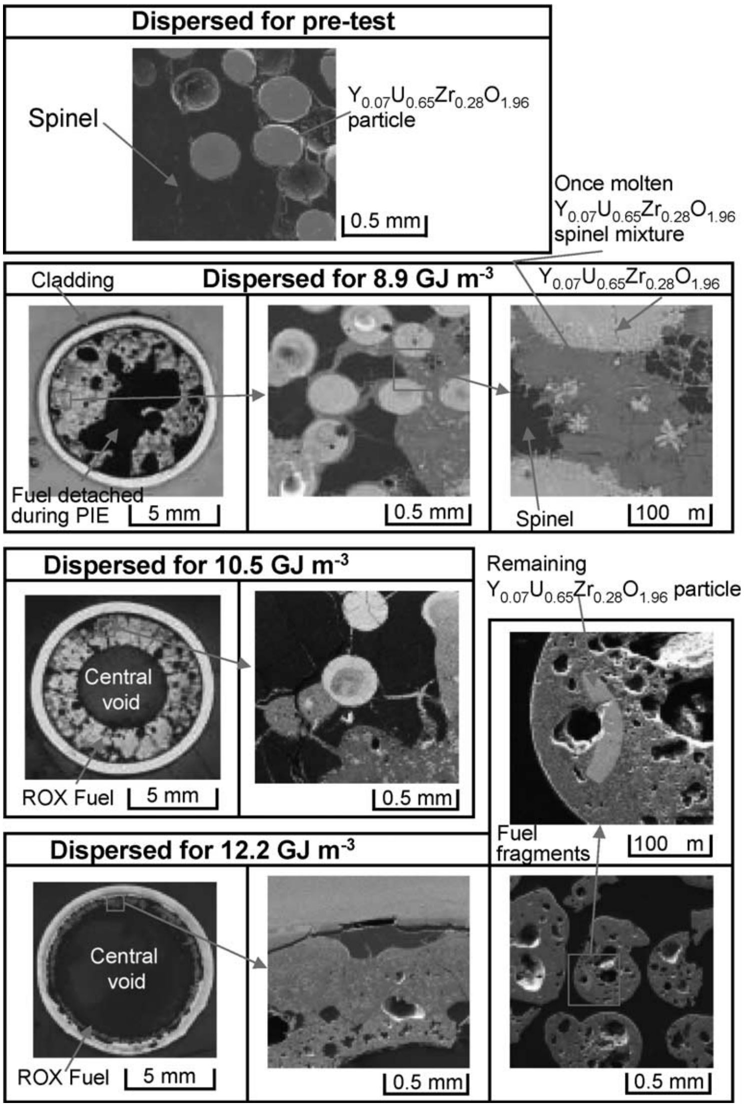

Fig. 7. Microstructure of the Dispersed type ROX fuel before and after the pulse irradiation tests. Interaction of $Y_{0.07}U_{0.65}Zr_{0.28}O_{1.96}$ particles with surrounding spinel ($MgAl_2O_4$) matrix was evident in the tests at peak fuel enthalpies of 8.9 GJ m^{-3} or higher.

could also reduce heat transfer to the coolant in a short term. In case of irradiated ROX fuel, on the other hand, much higher rod internal pressure is expected at the time of cladding failure, because of the fuel melting. Accordingly, more violent failure and enhanced fuel coolant mixing could generate the FCI for irradiated ROX fuel.

5. Conclusion

Pulse irradiation tests of three types of fresh ROX fuels were conducted in the NSRR. The ROX fuel rod failure occurred at peak fuel enthalpies above 10 $GJ\,m^{-3}$ (1.9 $kJ\,g^{-1}$), which was comparable to that of fresh UO_2 fuel (9.2 $GJ\,m^{-3}$ or 0.89 $kJ\,g^{-1}$) in volumetric enthalpy. The consequence of the ROX fuel rod failure, however, was quite different from that of UO_2 fuel, owing largely to their lower melting temperatures. Morphological change of the ROX fuels was examined by SEM/EPMA.

Interaction of the ROX fuel pellets and the cladding was evident at peak fuel enthalpies above 10 $GJ\,m^{-3}$, where cladding reached close to its melting temperature. Fuel melting due to interaction of UO_2–YSZ solid solution with spinel was evident at peak fuel enthalpies about 9 $GJ\,m^{-3}$ or higher in the composite type ROX fuel tests. Most part of the dispersed fuel fragments was made of once molten mixture of UO_2–YSZ solid solution and spinel. Average size of the ROX fragments was larger than those of fresh and irradiated UO_2 fuels that resulted in water hammer generation due to significant fuel–coolant interaction. Limited fuel and coolant mixing due to the low rod internal pressure and lower melting temperature in the ROX fuels should have contributed to the mechanically mild failure behavior of the ROX fuel rods.

Acknowledgements

The authors wish to thank colleagues in the NSRR Operation Division of JAERI for performing the test operations. High-quality work on the SEM/EPMA examinations by H. Nagashima and Y. Kimura of the Reactor Fuel Examination Division are greatly appreciated. They are grateful to K. Kusagaya, K. Okonogi and T. Yoshida for assisting the authors for conducting the post-test examinations and the data evaluation. The nuclear and thermal/mechanical calculations conducted by R. Hosoyamada are gratefully acknowledged.

References

[1] T. Yamashita, H. Kuramoto, H. Akie, Y. Nakano, N. Nitani, T. Nakamura, K. Kusagaya, T. Ohmichi, J. Nucl. Sci. Technol. 39 (2002) 865.
[2] H. Akie, T. Nakamura, Prog. Nucl. Energy 38 (2001) 363.
[3] N. Nitani, T. Yamashita, T. Matsuda, S. Kobayashi, T. Ohmichi, J. Nucl. Mater. 274 (1999) 15.
[4] K. Okonogi, T. Nakamura, M. Yoshinaga, K. Ishijima, H. Akie, H. Takano, J. Nucl. Mater. 274 (1999) 167.
[5] T. Nakamura, K. Kusagaya, M. Yoshinaga, H. Uetsuka, T. Yamashita, Prog. Nucl. Energy 38 (2001) 379.
[6] T. Nakamura, K. Kusagaya, H. Sasajima, T. Yamashita, H. Uetsuka, J. Nucl. Sci. Technol. 40 (2003) 30.
[7] L.J. Siefken, C.M. Allison, M.P. Bohn, S.O. Peck, FRAP-T6: a computer code for the transient analysis of oxide fuel rods, NUREG/CR-2148, EGG-2104, 1981.
[8] M. Ishikawa, S. Shiozawa, J. Nucl. Mater. 95 (1980) 1.
[9] T. Nakamura, H. Akie, K. Okonogi, M. Yoshinaga, K. Ishijima, H. Takano, Plutonium Rock-like Fuel Behavior under RIA Conditions, Workshop Proceedings of Advanced Reactors with Innovative Fuels, Villigen, Switzerland, 21–23 October 1998, p. 299.
[10] T. Fuketa, T. Fujishiro, Nucl. Eng. Design 146 (1994) 181.
[11] T. Nakamura, K. Kusagaya, T. Fuketa, H. Uetsuka, Nucl. Technol. 138 (2002) 246.
[12] T. Fuketa, F. Nagase, K. Ishijima, T. Fujishiro, Nucl. Safety 37 (1996) 4.
[13] Safety Evaluation Guidelines for Reactivity Initiated Events in Light Water Reactors for Power Generation, Nuclear Safety Commission of Japan, 1990.